RNA (2002), *8*:878–889. Cambridge University Press. Printed in the USA.

DOI: 10.1017.S1355838202029084

Translational feedback regulation of the gene for L35 in *Escherichia coli* requires binding of ribosomal protein L20 to two sites in its leader mRNA: A possible case of ribosomal RNA–messenger RNA molecular mimicry

MAUDE GUILLIER,[1] FRÉDÉRIC ALLEMAND,[1] SOPHIE RAIBAUD,[2] FRÉDÉRIC DARDEL,[2] MATHIAS SPRINGER,[1] and CLAUDE CHIARUTTINI[1]

[1]Institut de Biologie Physico-Chimique, Unité Propre de Recherche 9073 du Centre National de la Recherche Scientifique, Unité de Régulation de l'Expression Génétique chez les Microorganismes, 75 005, Paris, France
[2]Faculté de Pharmacie, Université Paris 5, Unité Mixte de Recherche 8015 du Centre National de la Recherche Scientifique, Laboratoire de Cristallographie et Résonance Magnétique Nucléaire biologiques, 75 006, Paris, France

ABSTRACT

In addition to being a component of the large ribosomal subunit, ribosomal protein L20 of *Escherichia coli* also acts as a translational repressor. L20 is synthesized from the IF3 operon that contains three cistrons coding for IF3, and ribosomal proteins L35 and L20. L20 directly represses the expression of the gene encoding L35 and the expression of its own gene by translational coupling. All of the *cis*-acting sequences required for repression by L20, called the operator, are found on an mRNA segment extending from the middle of the IF3 gene to the start of the L35 gene. L20-mediated repression requires a long-range base-pairing interaction between nucleotide residues within the IF3 gene and residues just upstream of the L35 gene. This interaction results in the formation of a pseudoknot. Here we show that L20 causes protection of nucleotide residues in two regions of the operator in vitro. The first region is the pseudoknot itself and the second lies in an irregular stem located upstream of the L35 gene. By primer extension analysis, we show that L20 specifically induces reverse transcriptase stops in both regions. Therefore, these two regions define two L20-binding sites in the operator. Using mutations and deletions of *rpmI'-'lacZ* fusions, we show that both sites are essential for repression in vivo. However L20 can bind to each site independently in vitro. One site is similar to the L20-binding site on 23S rRNA. Here we propose that L20 recognizes its mRNA and its rRNA in similar way.

Keywords: feedback regulation; molecular mimicry; mRNA; ribosome; rRNA; translation

INTRODUCTION

In bacteria, the genes for ribosomal proteins (r-proteins) are clustered, and probably, as was shown to be the case in *Escherichia coli*, expressed as operons. In this bacterium, the expression of r-proteins is often feedback regulated at the translational level by one of the operon products that binds to its own mRNA at a site called the operator. Based on the apparent similarities between some of the r-protein translational operators in mRNAs and their binding sites on rRNA, Nomura et al. (1980) proposed that the regulatory r-proteins recognize both sites similarly. More importantly, it was hypothesized that a regulatory r-protein preferentially binds to its primary target, rRNA, and under conditions where rRNA sites are all occupied, it binds to the operator site on its own mRNA to block its own synthesis. This notion of "mimicry" between two binding sites present on rRNA and mRNA has been convincingly demonstrated in the case of the L11-L1 operon (Nomura et al., 1984; Zengel & Lindahl, 1994). In this operon, r-protein L1 directly down-regulates the expression of the gene encoding r-protein L11, and regulation is transmitted to the downstream L1 cistron by translational coupling.

Reprint requests to: Claude Chiaruttini, Institut de Biologie Physico-Chimique, Unité Propre de Recherche 9073 du Centre National de la Recherche Scientifique, Unité de Régulation de l'Expression Génétique chez les Microorganismes, 13, rue Pierre et Marie Curie, 75 005, Paris, France; e-mail: chiaru@ibpc.fr.

Abbreviations: CMCT: 1-cyclohexyl-3-(β-morpholinyl-(4)-ethyl)-carbodiimide-methyl-*p*-toluene sulfonate; DMS: dimethylsulfate; IF3: translation initiation factor 3; iris: *infC-rpmI* intergenic spacer; RT: reverse transcriptase; SD: Shine–Dalgarno sequence; ThrRS: threonyl-tRNA synthetase.

The operator located upstream of the L11 cistron and the L1-binding site on 23S rRNA show similar structures, and changes in equivalent nucleotide residues of each site were shown to have analogous effects, that is, changes in the operator decrease repression by L1, whereas those in the L1-binding site on 23S rRNA reduce its ability to titrate L1 in vivo (Said et al., 1988). Although mimicry in this case is quite convincing, it should, however, be noted that L1 binding to the operator has not yet been reported in *E. coli*. In vitro binding of L1 to its rRNA and mRNA binding sites has been demonstrated in the case of the archaeon *Methanococcus vannielii*, although the organization of the operon regulated by L1 is quite different from that of the *E. coli* L11-L1 operon (Köhrer et al., 1998). Mimicry probably also occurs in the case of the *spc* operon. In this case, the regulatory r-protein S8 directly represses the expression of the third cistron. The operator is located between the second and the third cistrons of the operon. Filter binding and RNase footprinting studies have shown that S8 binding sites on 16S rRNA and mRNA are similar (Gregory et al., 1988). In vitro assays of S8 binding to either 16S rRNA or operator RNA fragments of decreasing sizes have shown that the "minimal" operator, that is, the shortest operator for which the affinity for S8 remains unchanged, has about a fourfold lower affinity for S8 than the rRNA-binding site (Wu et al., 1994). Changes in the rRNA site that increases its resemblance to the operator site were shown to decrease the affinity for S8 to the same level as that of mRNA and vice versa. Finally, S8 mutants selected for their inability to repress translation of the *spc* operon (Wower et al., 1992) showed decreased affinity for 16S rRNA (for review, see Springer et al., 1998). At the present time, no clear-cut mimicry between the primary function of the regulating protein, that is, participation in ribosome assembly, and regulation has been demonstrated for most of the other r-protein genes that are down-regulated by translational feedback.

This work deals with the IF3 operon containing the *infC*, *rpmI*, and *rplT* genes, encoding IF3 and the two ribosomal proteins, L35 and L20, respectively. Expression of the IF3 operon is regulated by two different control loops, both acting at the translational level. First, IF3 represses the expression of its own gene (Butler et al., 1986). Second, L20 directly represses the expression of *rpmI*, and indirectly that of its own gene, *rplT*, through translational coupling with *rpmI* (Lesage et al., 1992). We have previously shown that the *rpmI* translational operator, defined as the *cis*-acting mRNA sequences required for L20-mediated repression of *rpmI* expression, contains two distantly located sets of nucleotides that base pair to form a double-stranded structure, called stem S2, that is crucial to the formation of a pseudoknot required for repression (Chiaruttini et al., 1996). Here, we present results obtained using a combination of in vitro and in vivo approaches, which indicate that L20 recognizes two binding sites in the operator. The first site is delineated by the pseudoknot. The second site is located in the middle of an irregular stem-loop structure located between the two strands of stem S2. The structure of this site is similar to that of the putative L20-binding site on *E. coli* 23S rRNA, as deduced from the high resolution structure of the large subunit from *Deinococcus radiodurans* (Harms et al., 2001). Finally, we also discuss the possible implication of our results on the way L20 interacts with both 23S rRNA and the *rpmI* translational operator.

RESULTS

In vitro footprinting of the *rpmI* translational operator with base-specific chemical probes

We examined the reactivity of transcripts containing the *rpmI* translational operator against the base-specific chemical probes DMS and CMCT, both in the absence and in the presence of L20. In this experiment, a transcript containing a shortened form of the *rpmI* translational operator was incubated with a 30-fold molar excess of L20 prior to addition of the chemicals, and used as a template for primer extension. This shortened form of the operator was constructed by deleting nucleotide residues from positions infC A365 to infC C521 (see Fig. 1), and was previously shown to contain all the sequences required for repression (Chiaruttini et al., 1996). Modified nucleotide residues were identified by primer extension assays using two oligodeoxynucleotide primers complementary to either the translation initiation site or an internal sequence of *rpmI*. When L20 was added, an extensive set of protections was observed compared to the transcript in the absence of L20 (Fig. 2, Table 1). No enhancement of reactivity was observed. All of the L20-induced protections were confined to two regions of the *rpmI* translational operator (Fig. 1, Table 1). The first region is delineated by the upper half of stem S1 (residue infC C318) and the two strands of stem S2 (infC U332, C336, and A337 and iris U76 and A81). This region is located within the pseudoknot (Fig. 1, inset B). The second region contains the central part of stem t_1 (infC U541 and iris C52). Protected residues are also located in the 4-nt region bridging stems t_1 and S2 (iris C73, A74, and A75) and in stem S3 (rpmI U2), which stacks onto stem S2 in the pseudoknot (Chiaruttini et al., 1996). However, all of these regions are brought into close proximity in the context of the pseudoknot; thus all the protected residues are confined to a single region in the three-dimensional structure of the operator.

In vitro footprinting of the *rpmI* translational operator with iodine

Footprinting experiments were performed on phosphorothioate-substituted transcripts containing the short-

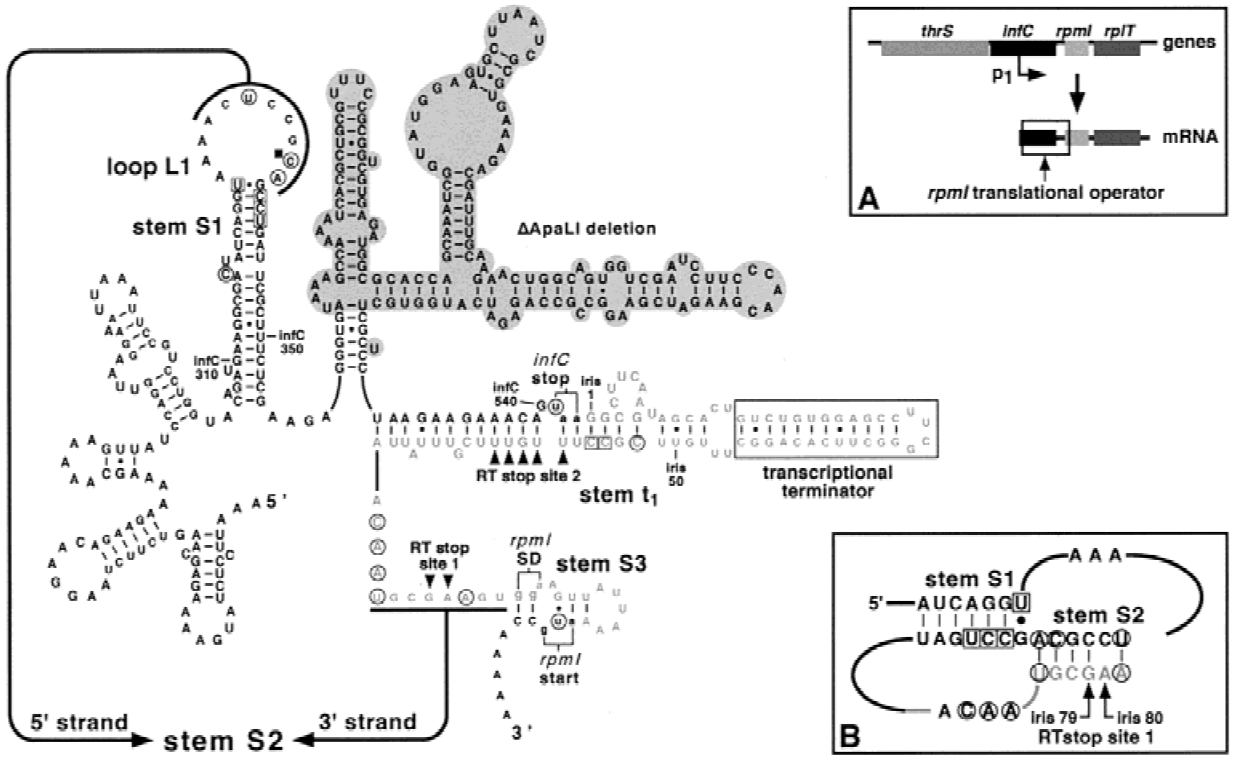

FIGURE 1. Localization of the nucleotide residues protected in footprinting experiments and of the L20-induced RT stop sites. The model of the secondary structure of the *rpmI* translational operator is taken from a previous work (Chiaruttini et al., 1996). A schematic description of the IF3 operon preceded by *thrS* and the localization of the *rpmI* translational operator on the mRNA are presented in inset A. Residues protected from DMS and CMCT modification are circled and those protected from iodine cleavage are boxed. Residue infC C336, showing enhancement of reactivity toward iodine cleavage, is indicated by a filled square. The relevant features of the operator (stem S1, loop L1, stems S2 forming the pseudoknot, S3 and t_1 containing the boxed t_1 transcriptional terminator) are also indicated. A simplified scheme of the pseudoknot without stem S3 is shown in inset B. The long-range interaction forming stem S2 holding the pseudoknot is schematized by arrows. The *infC* stop codon and the *rpmI* SD and start codon sequences are in lowercase. The ΔApaLI deletion is boxed in gray. RT stops defining RT stop sites 1 and 2 are indicated by arrowheads. Coding sequences for *infC* and *rpmI* and iris sequences are in black and gray, respectively.

ened form (see above) of the *rpmI* translational operator, both in the absence and in the presence of L20. Iodine cleavages of the RNA backbone were revealed by primer extension assays using the same pair of oligodeoxynucleotide primers employed above. In the presence of L20, the relative intensity of only a few bands was decreased in comparison to the pattern obtained in the absence of the protein, thus revealing local protection of phosphate groups upon addition of L20 (Fig. 3, Table 1). Protections were found in the same regions as those identified by footprinting with base-specific chemical probes (Fig. 1), that is, the pseudoknot (residues infC C339, C340, and U341) and the central part of stem t_1 (residues iris C54 and C55). We observed an enhancement of cleavage at position infC C336 in the first region (Fig. 3, Table 1). This nucleotide is located in the 5′ strand of stem S2 and is located very close to residues protected from iodine cleavage in the upper part of stem S1 (Fig. 1). It is possible that this enhancement of reactivity could be accounted for by local rearrangement of the RNA backbone in the vicinity of the phosphate groups that contact L20. It should be noted that this residue is also protected from the base-specific probe CMCT (Fig. 1).

L20 induces RT stops in the *rpmI* translational operator in vitro

L20 interaction with the shortened form (see above) of the *rpmI* translational operator was also investigated using primer extension of an oligodeoxynucleotide primer complementary to a sequence internal to *rpmI*, either in the absence or in the presence of the protein. Gel electrophoresis of the extended primer shows that L20-induced stops occur in two sites upstream of *rpmI* (Fig. 4). The appearance of these bands is not due to some nuclease activity displayed by the protein, because they disappear after proteinase K treatment and phenol extraction of the chemically modified transcripts in the presence of L20 (Fig. 2; data not shown). Stops at positions iris G79 and iris A80 define RT stop site 1 located in the pseudoknot (Figs. 1 and 4). Stops at

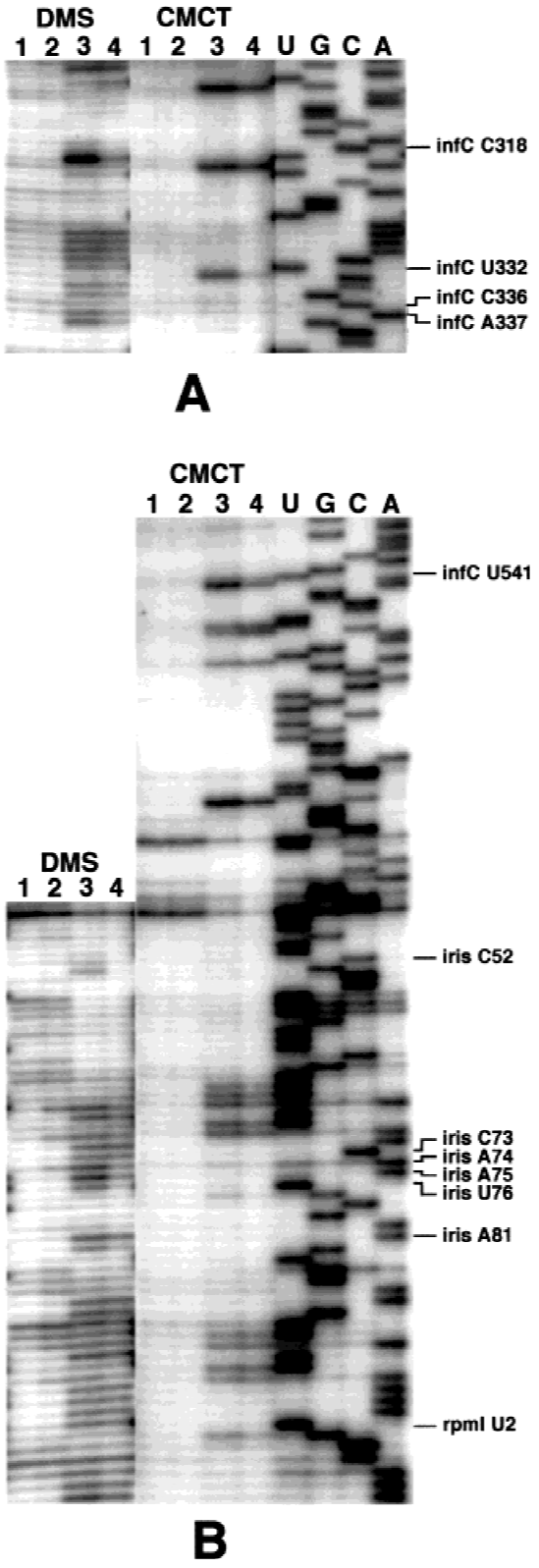

FIGURE 2. Results of DMS and CMCT modification of the *rpmI* translational operator following incubation either in the absence or in the presence of L20. Lane 1: unmodified operator; lane 2: unmodified operator plus L20; lane 3: modified operator; lane 4: modified operator plus L20. U, G, C, A are sequencing lanes. Only those residues exhibiting differences in reactivities in the absence and in the presence of L20 are indicated on the right of each gel. **A:** Extension of the rpmI SD primer. **B:** Extension of the rpmI84 primer.

positions iris U57, iris U58, iris G59, iris U60, and iris U61 define RT stop site 2, located immediately to the left of the region in stem t_1 protected in the footprinting experiments (Figs. 1 and 4). Stops at the same positions were obtained when a transcript containing the full-length wild-type translational operator was used (data not shown). In a control experiment, in which the *thrS* translational operator was used as a template, no primer extension stops appeared upon addition of L20 (Fig. 4). In another control experiment, we also showed that the L20-induced stops could not be observed upon addition of another RNA-binding translational repressor, ThrRS (data not shown). Interestingly, upon formation of stem S2, RT stop site 1 is brought just downstream of nucleotide residues protected from iodine cleavage in the apical half of stem S1 (Fig. 1, inset B). It is also worth noting that RT stop site 2 lies just downstream of nucleotide residues protected from iodine cleavage in the central region of stem t_1 (Fig. 1). However, from these results, it was not possible to determine whether or not the two RT stop sites were generated from the same transcript. We reasoned that if increasing amounts of L20 were added, we should observe the disappearance of bands at RT stop site 2 because RT should have been arrested at site 1 on each transcript molecule. Although L20 was used in a 30-fold molar excess over transcript, complete primer extension arrest was far from being achieved, since the major extension product was full-length cDNA (Fig. 4). Unfortunately, in our reaction conditions, further addition of L20 results in a dramatic inhibition of the extension reaction, thus precluding any further analysis. This inhibition is most probably due to nonspecific binding of L20, an extremely basic protein, to RNA.

Effect of deletions and mutations in the stem S1-loop L1 structure

The results from the iodine footprinting experiments on phosphorothioate-substituted transcripts identified protected nucleotide residues in the stem S1-loop L1 structure (Table 1; Figs. 1 and 3). First, we investigated the effect of a series of deletions in this stem-loop on the repression of *rpmI'-'lacZ* fusions in vivo. In agreement with previous results from a mutational analysis showing that the upper half of this stem-loop structure contains nucleotide residues required for repression (Chiaruttini et al., 1996), deletion of the uppermost 5 bp of stem S1 and loop L1 (deletion 1) resulted in more than a 15-fold decrease in repression (Fig. 5). Specific features contained in that region were also shown to be crucial, because deletion of the 5′ strand of stem S2 (deletion 2) or the uppermost 5 bp of stem S1 (deletion 3) resulted in more than a 15-fold and a 10-fold decrease in repression, respectively. We also specifically made a deletion of the two nucleotide residues bulged at positions infC 318 and infC 319 (deletion 4), be-

TABLE 1. Relative reactivities of bases and phosphate groups in transcripts containing the *rpmI* translational operator incubated both in the absence and in the presence of L20.[a]

Nucleotide residue	Region	Operator	Operator + L20
infC C318 (base)	(stem S1, pseudoknot)	+++	+/−
infC U332 (base)	(stem S2, pseudoknot)	++	+/−
infC C336 (base)	(stem S2, pseudoknot)	+	+/−
(phosphate group)		+	+++
infC A337 (base)	(stem S2, pseudoknot)	+	+/−
infC C339 (phosphate group)	(stem S1, pseudoknot)	++	+
infC C340 (phosphate group)	(stem S1, pseudoknot)	++	+/−
infC U341 (phosphate group)	(stem S1, pseudoknot)	+	0
infC U541 (base)	(stem t_1)	+++	+
iris C52 (base)	(stem t_1)	+/−	0
iris C54 (phosphate group)	(stem t_1)	+++	+
iris C55 (phosphate group)	(stem t_1)	+++	+
iris C73 (base)	(stem t_1-stem S2 bridge)	+	+/−
iris A74 (base)	(stem t_1-stem S2 bridge)	++	+/−
iris A75 (base)	(stem t_1-stem S2 bridge)	+	0
iris U76 (base)	(stem S2, pseudoknot)	+/−	0
iris A81 (base)	(stem S2, pseudoknot)	+	0
rpmI U2 (base)	(stem S3, pseudoknot)	+	+/−

[a]Bases are modified using DMS for adenines and cytosines and CMCT for guanines and uracils. Phosphate groups are probed using iodine cleavage on phosphorothioate-substituted transcripts. Nucleotide residues are listed according to their positions in the 5′-to-3′ orientation. The regions containing the protected residues are described in the text. Data correspond to Figures 2 and 3 and are the consensus of visual estimates of relative band intensities from two different probing experiments at least. Reactivities are summarized by the symbols 0, +/−, +, ++, and +++, where 0 indicates no reactivity, and +++ indicates maximal reactivity. Data are indicated only for those nucleotide residues which exhibit different reactivities in the absence and in the presence of L20.

cause the chemical footprinting experiments indicated that residue infC C318 was the residue most protected in the presence of L20 (Table 1, Fig. 2). Our results show that deletion of both residues does not affect repression (Fig. 5), thus indicating that they are not required for repression. This result indicates that footprinting data using base-specific chemical probes must be interpreted with caution because they primarily reflect conformational alterations of RNA structure induced by the protein. Finally, flipping the uppermost 5 bp of stem S1 by changing each nucleotide residue to its complement (mutation 7) did not affect repression, whereas destabilization of this 5-bp segment by changing each strand of the segment individually (mutations 5 and 6) caused a fourfold and sevenfold reduction in repression, respectively (Fig. 5). This result suggests that the double-stranded nature of the upper part of stem S1, but not its sequence, is crucial to repression.

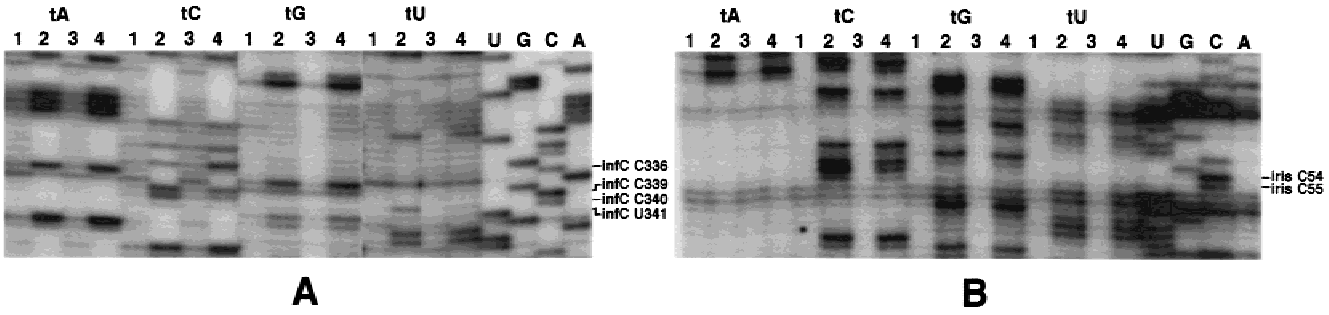

FIGURE 3. Results of iodine cleavage of the *rpmI* translational operator following incubation of the four phosphorothioate-substituted transcripts either in the absence or in the presence of L20. The S_p diastereomer of NTP[αS] incorporated into the transcripts is indicated on top of the lanes. tA, tC, tG, and tU are the lanes for transcripts substituted with ATP[αS], CTP[αS], GTP[αS], and UTP[αS], respectively. Lane 1: no iodine, no L20; lane 2: plus iodine, no L20; lane 3: no iodine, plus L20; lane 4: plus iodine, plus L20. U, G, C, A are sequencing lanes. Only those residues exhibiting differences in reactivities in the absence and in the presence of L20 are indicated on the right of each gel. **A:** Extension of the rpmI SD primer; **B:** Extension of the rpmI84 primer.

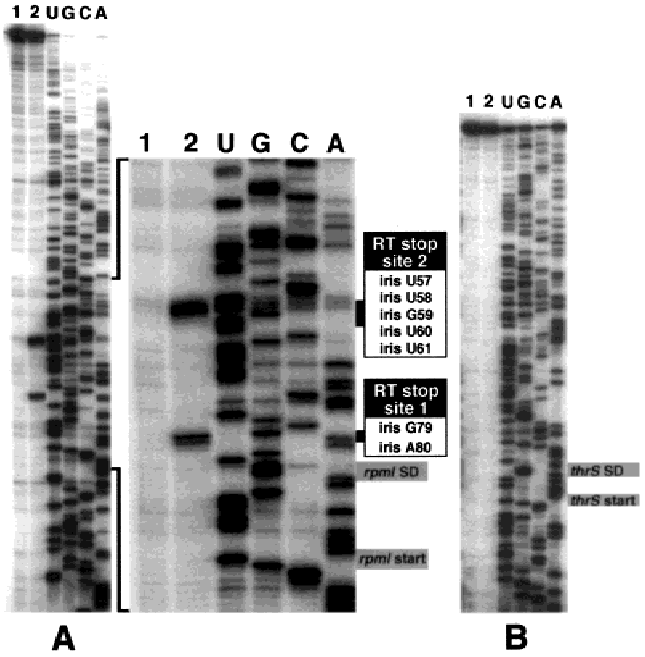

FIGURE 4. Localization of the L20-induced RT stops on the *rpmI* translational operator. Lane 1: operator; lane 2: operator plus L20. U, G, C, A are sequencing lanes. **A:** Extension of the rpmI84 primer using the *rpmI* translational operator as template. A magnified view of the gel around RT stop sites is shown. The positions of the L20-induced stop sites are boxed. **B:** Extension of the M13 17-mer primer using the *thrS* translational operator as template. The SD and start codon sequences for both *rpmI* and *thrS* are indicated on the right of the corresponding gel.

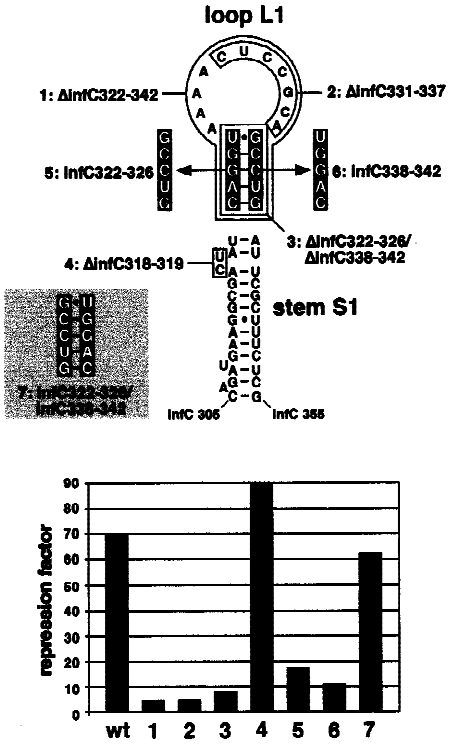

FIGURE 5. Effect of deletions and mutations in the stem S1-loop 1 structure on L20-mediated repression. Deletions and point mutations are represented by open and filled boxes, respectively. The *rpmI'-'lacZ* translational fusion cloned into λ bacteriophage was integrated into the chromosome of *E. coli* IBPC5311 and the lysogen was transformed either by pBR322 or by pBL6. The repression factor is calculated as the ratio of the β-galactosidase activity assayed in the presence of control plasmid pBR322 to the activity assayed in the presence of the L20-overproducing plasmid pBL6. The repression factors are expressed below the schematic diagram of the stem S1-loop L1 structure as histograms, numbered according to the corresponding deletion or mutation shown on the diagram.

Effect of mutations in stem t_1

Our results showing that RT stop site 2 occurs just downstream of residues protected from iodine cleavage in the central region of stem t_1 (Figs. 1 and 4) prompted us to analyze the effect of mutations in that region in vivo. Because RT stop site 2 is located immediately downstream of the two G-C base pairs, iris G1-iris C55 and iris G2-iris C54 (Fig. 1), we suspected them to be crucial for repression, either because they are stabilized by L20 and/or because they are involved in L20 binding. The contribution of this base pair doublet to repression was investigated in vivo by mutagenesis of *rpmI'-'lacZ* fusions containing the full-length *rpmI* translational operator. Disrupting base pairs iris G1-iris C55 and iris G2-iris C54 either by replacing the G nucleotide residues at positions iris G1 and iris G2 with A residues (mutation 1) or by replacing the two C nucleotide residues at positions iris C54 and iris C55 with U residues (mutation 2) resulted in a three- to fourfold decrease in repression for both changes (Fig. 6). Flipping both mutations in order to restore base pairing (mutation 3) reestablishes repression to a level even higher than that of the wild-type fusion (102.5 vs. 73.2; Fig. 6). This result suggests that the double-stranded nature of the central part of stem t_1, but not its sequence, is crucial to repression. Base pairing of the nucleotide residues lying immediately to the left of this base pair doublet is not critical, because mutations therein have either no (mutation 4) or a limited effect (mutation 5) on repression (Fig. 6). The contribution of sequences located to the right of the base pair doublet to repression was tested using two deletions of increasing sizes (deletions 6 and 7) in the apical part of stem t_1 (Fig. 6). Both deletions resulted in a 10-fold decrease in repression, indicating that the G-C base pair doublet is crucial for repression, together with sequences located to the right of the 6-nt CUUCAA internal loop of stem t_1.

Minimum sequences of the *rpmI* translational operator required for repression

Our findings that (1) RT stop sites 1 and 2 fall squarely in the pseudoknot and the left half of stem t_1, respectively, and (2) both sites are located just downstream of nucleotide residues protected by L20 in iodine footprint-

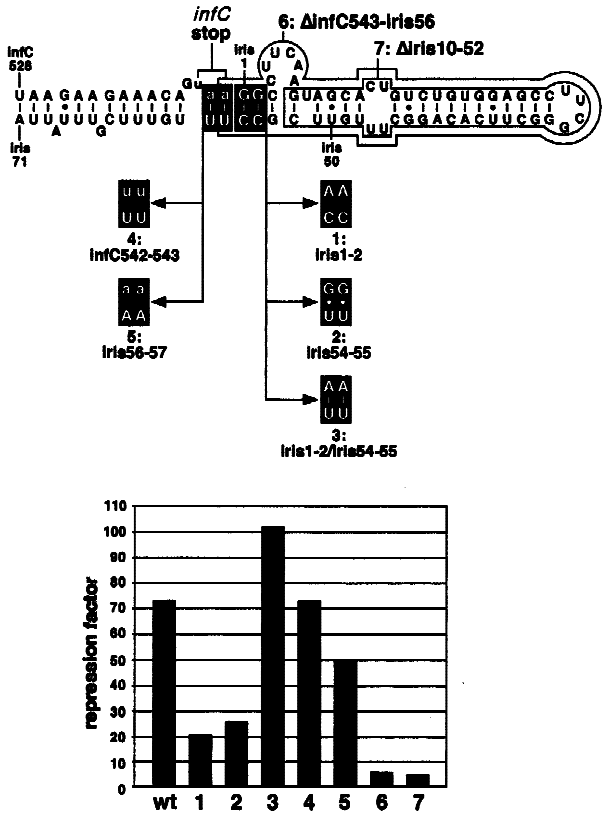

FIGURE 6. Effect of mutations and deletions in stem t_1 on L20-mediated repression. Deletions and point mutations are represented by open and filled boxes, respectively. The sequence of the *infC* stop codon is indicated in lowercase. Repression was assayed and the repression factors were calculated as indicated in the legend to Figure 5. The repression factors are expressed below the schematic diagram of stem t_1 as histograms, numbered according to the corresponding deletion or mutation shown on the diagram.

ing experiments (Fig. 1) prompted us to look at the effect of deletions outside of the stem S1-loop L1 structure and stem t_1 in vivo. The effect of individual deletions of specific stem-loop structures on the repression of *rpmI'-'lacZ* fusions was assayed (Fig. 7). When we started these experiments, we were already aware that deletion of the sequences located between stems S1 and t_1 (Fig. 7) did not affect repression (Chiaruttini et al., 1996). The results in Figure 7 show that the sequences located upstream of stem S1 are not required for repression either, because deletions Δ1, Δ2, Δ3, and Δ4 give repression levels quite similar to that of the wild-type operator. The contribution of the most apical part of stem t_1 to repression was tested by using deletion Δ5, which removes the t_1 transcriptional terminator (Fig. 7). Clearly, this deletion does not affect repression, thus indicating that the terminator is not involved in control by L20. Therefore, the "minimal" *rpmI* translational operator, that is, the sequences required for repression, is restricted to the stem S1-loop L1 structure, stem t_1 minus the t_1 transcriptional terminator, and the sequences just upstream of *rpmI*. This minimal operator overlaps the pseudoknot and the left two-thirds of stem t_1, the two regions where L20-induced protections and RT stop sites 1 and 2 have been localized (compare Figs. 1 and 7).

L20 binds to two sites of the *rpmI* translational operator independently

L20 interaction with the *rpmI* translational operator was further investigated using the L20-induced primer extension arrest assay described above. In this experiment, we used transcripts spanning the full-length operator and examined the effect of two mutations that were shown to strongly decrease repression in vivo because they prevent either the formation of the pseudoknot or base pairing in the central part of stem t_1. The pseudoknot was disrupted by deleting the 5′ strand of stem S2 (deletion ΔinfC331–337 in Fig. 8). Base pairing in the central part of stem t_1 was disrupted by mutating the three G-C and C-G base pairs from positions iris G1 to iris C3 and positions iris G53 to iris C55 (mutation iris 53–55 in Fig. 8). L20 induces stops at RT stop sites 1 and 2 with the wild-type operator (Fig. 8, lane 2). Disruption of the pseudoknot with deletion ΔinfC331–337 (mutation 1) leads to a disappearance of the bands corresponding to RT stop site 1 (Fig. 8, lane 4). This deletion results in an almost 20-fold reduction of repression in vivo (repression factor 73.2 for the wild-type fusion vs. 3.9 for the deleted fusion). In contrast, the bands corresponding to RT stop site 2 are maintained. Abolishing base pairing in the central part of stem t_1 with mutation iris 53–55 (mutation 2) results in the disappearance of bands corresponding to RT stop site 2 (Fig. 8, lane 6). This mutation results in a 10-fold decrease in repression in vivo (repression factor 73.2 for the wild-type fusion vs. 7.7 for the mutated fusion). In contrast, the bands corresponding to RT stop site 1 are preserved. These results suggest that L20 is able to bind the nucleotide residues located upstream of RT stop sites 1 and 2, independently.

DISCUSSION

The *rpmI* translational operator has two L20-binding sites

We show here by in vitro footprinting and primer extension assays using transcripts on the *E. coli rpmI* translational operator, that L20 probably recognizes two sites in the operator. Protection experiments performed with base-specific chemical probes allowed us to identify two regions of the operator in which the protected nucleotide residues are clustered (Fig. 1). The first region contains the pseudoknot formed by the stacking of stem S2 onto stem S1, which we have previously shown to be required for repression (Chiaruttini et al., 1996). The second region lies within an irregular stem-loop

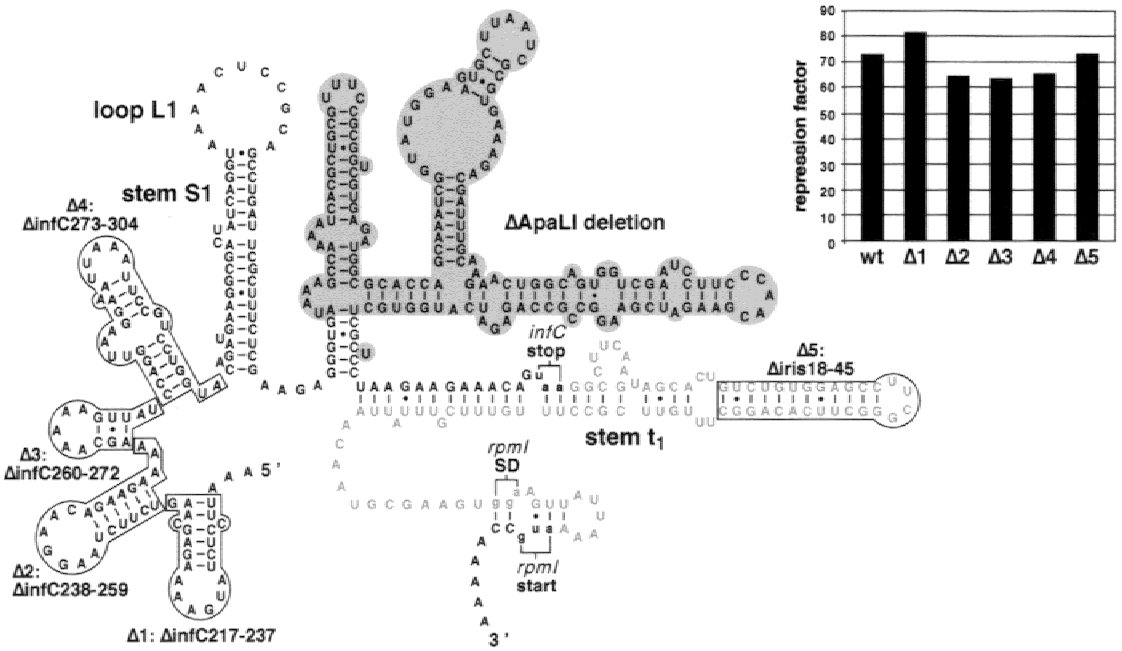

FIGURE 7. Effect of deletions in the *rpmI* translational operator on L20-mediated repression. Deletions introduced in this work are within open boxes. Deletion ΔApaLI is shown within the gray box and was found not to affect repression (Chiaruttini et al., 1996). The *infC* stop codon and the *rpmI* SD and start codon sequences are indicated in lowercase. Coding sequences for *infC* and *rpmI* and iris sequences are in black and gray, respectively. Repression was assayed and the repression factors were calculated as indicated in the legend to Figure 5. The repression factors are expressed to the right of the figure as histograms, numbered according to the corresponding deletion on the secondary structure model of the *rpmI* operator.

structure called stem t_1, located between the two distantly located strands of stem S2 (Fig. 1). Both regions are defined by nucleotide residues that are protected in iodine cleavage footprinting experiments using phosphorothioate-substituted transcripts by the presence of L20 (Fig. 1). This suggests that L20 contacts both regions through interaction with the phosphate groups of the protected residues. Finally, primer extension experiments identified two sites of RT stops, which prevent the enzyme from extending the nascent cDNA farther upstream. We presume that these roadblocks are caused by L20 itself. Each of these two sites lies squarely in the regions containing protected residues. RT stop site 1 falls in the 3′ strand of stem S2. In the pseudoknot, stem S2 is brought into close proximity with nucleotide residues of the upper part of stem S1, which are protected by L20 against iodine cleavage (Fig. 1, inset B). Presumably, L20 bound to the upper part of stem S1 blocks RT on the 3′ strand of stem S2 resulting in two bands corresponding to RT stops at this position. RT stop site 2 lies in the central part of stem t_1 and lies immediately downstream of nucleotide residues protected by L20 against iodine cleavage. As in the case of RT stop site 1, arrest of primer extension at RT stop site 2 is probably due to binding of L20. Therefore, the two sites define two L20-binding sites in the *E. coli rpmI* translational operator in vitro. The presence of these two binding sites was confirmed in vivo by analyzing the effect of mutations and deletions on the repression of *rpmI'-'lacZ* translational fusions. By mutational analysis we had previously identified the pseudoknot, resulting from base pairing interaction of two distantly located sets of nucleotides in the operator, as a site required for repression (Chiaruttini et al., 1996). We show here that mutations in the central part of stem t_1 strongly decrease L20-mediated down-regulation of *rpmI* expression as well (Fig. 6), thus identifying a second site crucial for repression.

The regions located outside of the pseudoknot and the lower part of stem t_1 are not critical for repression, as deletions of all of the sequences upstream of stem S1 and in the apical region of stem t_1 have no or little effect on control (Fig. 7). In addition, we have previously shown that the sequences located between the two stems are not required either (Chiaruttini et al., 1996). Therefore, the minimal operator, absolutely required for repression, comprises the pseudoknot and the lower two-thirds of stem t_1, the two regions of the operator containing the L20-binding sites.

One important finding is that the nucleotide sequences of the two regions containing phosphate groups contacting L20 are not important in down-regulating the expression of *rpmI'-'lacZ* fusions. Flipping the five uppermost base pairs of stem S1 has no effect on repression (Fig. 5). The same is true when the two iris G1-iris C55 and iris G2-iris C54 base pairs in the central part

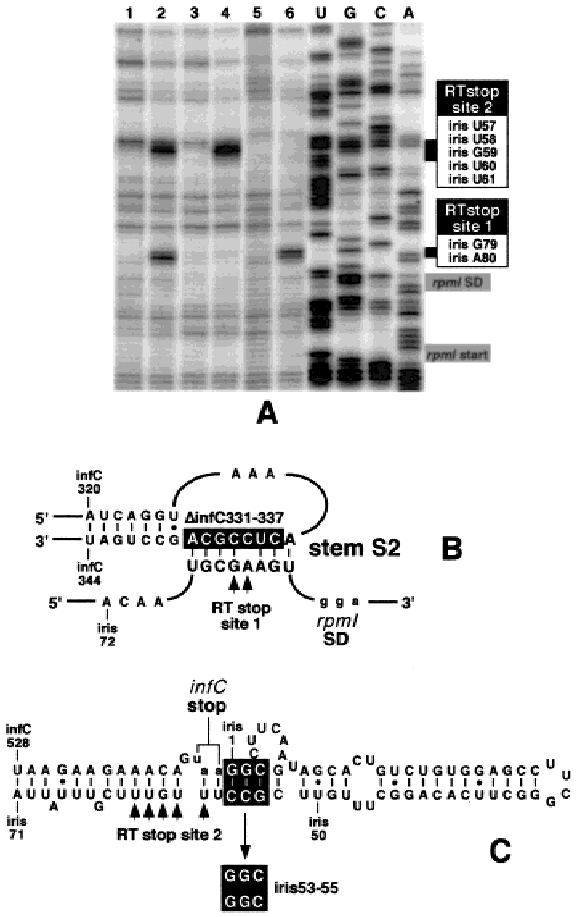

FIGURE 8. Effect of mutations on L20-induced RT stops. **A:** Electrophoretic analysis of RT extension products using the rpmI84 primer. Lane 1: wild-type operator; lane 2: the same as in lane 1 plus L20; lane 3: operator carrying the deletion ΔinfC331–337; lane 4: the same as in lane 3 plus L20; lane 5: operator carrying the mutation iris53–55; lane 6: the same as in lane 5 plus L20. U, G, C, A are sequencing lanes. The positions of RT stop sites 1 and 2 are boxed to the right of the gel. **B:** Schematic diagram of the pseudoknot. **C:** Schematic diagram of stem t_1. Both deletion and mutation are within filled boxes. The positions of RT stop sites 1 and 2 are indicated by arrowheads.

of stem t_1 are substituted with A-U base pairs (Fig. 6). Therefore, it is likely that L20 interacts with both regions, in part by contacting the RNA backbone of the operator in a sequence-independent manner. Furthermore, these compensatory changes demonstrate that both stems must form in order for L20 to bind. Presumably, the helical structure of these two specific regions of the operator dictates the phosphodiester-backbone structure required for L20 binding.

A possible case of mimicry

Recent determination of the three-dimensional structure of the large ribosomal subunit of *D. radiodurans* allowed us to clearly identify 23S rRNA helices H40 and H41 as probable sites of L20 contact (Harms et al., 2001). The same site has been identified by fitting the three-dimensional structure of the globular C-terminal half of L20 from *Aquifex aeolicus*, determined by NMR studies, to the electron density map of the *Thermus thermophilus* ribosome (S. Raibaud, I. Lebars, M. Guillier, C. Chiaruttini, F. Bontems, A. Rak, M. Garber, F. Allemand, M. Springer, and F. Dardel, submitted). Interestingly, the overall structure at the junction between helices H40 and H41 of 23S rRNA is similar to that at the junction between the two helices of binding site 2 on the operator (Fig. 9). Both structures exhibit a certain number of additional similarities. In particular, both contain common residues at identical positions, a 6-nt internal loop ending with two 3′ A residues and a bulged U residue between the two lower base pairs of the upper helix (Fig. 9). From the results of current mutational analysis, we already know that the two conserved A residues that terminate the 6-nt internal loop of binding site 2 are critical for repression (M. Guillier, unpubl. results). The N_3 of the A residue located at the 3′ end of the loop present in 23S rRNA from *D. radiodurans* interacts by hydrogen bonding with the N_2 of the G residue of the second base pair from the top of helix H40 (Fig. 9). It is possible that the same kind of interaction takes place in L20 binding site 2 on the operator, thus suggesting that this A residue could either be recognized as a specific determinant by L20 directly or could contribute to binding of the protein by inducing the formation of a specific structural motif in the RNA backbone, which, in turn, would be recognized by L20. Further mutational analysis is needed to address the role of the common specific residues in L20-binding sites on the operator and 23S rRNA.

How many L20 molecules bind to the operator?

Disrupting the L20 binding site 1 on the operator with deletion ΔinfC331–337, which prevents the formation of stem S2, or site 2, with mutation iris 53–55, which breaks the central part of stem t_1, results in a seven- and ninefold decrease in repression, respectively. This indicates that both binding sites are required for down-regulation of the *rpmI'-'lacZ* fusions in vivo, as mutation of only one site is sufficient to strongly decrease repression. However, the results of primer extension assays in vitro show that disruption of the first binding site does not prevent RT arrest at the second site and vice versa, suggesting that L20 binds to each site independently (Fig. 8). One implication of this observation is that binding of L20 to one site does not contribute to the formation of the other L20 binding site on the operator. If we consider these in vivo and in vitro results together, we can address the question of how many L20 molecules bind to the operator. The presence of two independent binding sites in the operator and the lack of symmetry in the L20 protein structure (Harms

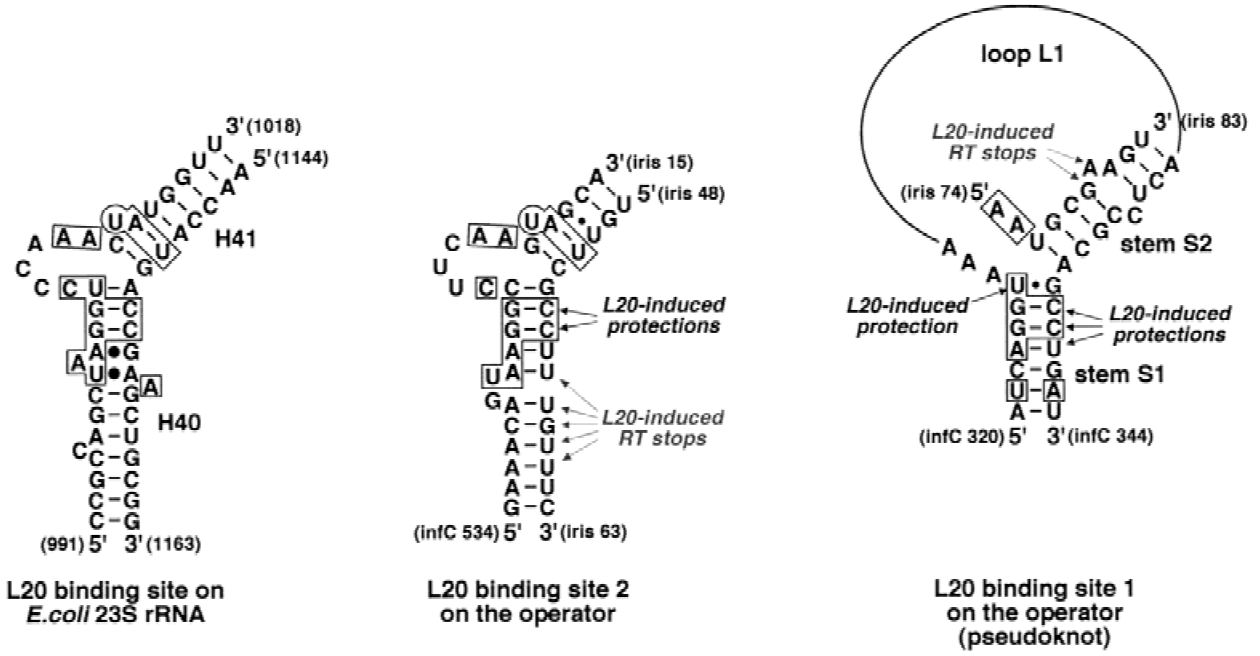

FIGURE 9. Secondary structures of the L20-binding sites on *E. coli* 23S rRNA and *rpmI* translational operator. The putative L20 binding site on *E. coli* 23S rRNA was deduced from the L20-binding site on 23S rRNA in the large ribosomal subunit of *D. radiodurans* (Harms et al., 2001). Canonical and G.U base pairings are indicated by thin lines and small dots, respectively. Noncanonical base pairings are indicated by large dots. Numbering of the terminal nucleotide residues on each strand of L20-binding site on 23S rRNA is that of *E. coli* 23S rRNA. Regions of L20-binding sites on *E. coli* 23S rRNA and the operator exhibiting sequence similarity are boxed. Nucleotide residues containing phosphate groups protected by L20 in iodine footprinting experiments are indicated by black arrows. RT stop sites 1 and 2 are indicated by gray arrows. The relevant features of the pseudoknotted structure of L20-binding site 1 (stems 1 and 2 and loop L1) are indicated.

et al., 2001; Raibaud et al., submitted), which a priori excludes the possibility that a single L20 molecule contains two identical RNA-binding sites, suggests that the answer is two. This scenario is particularly true if L20 recognizes both operator sites 1 and 2 similarly. However, despite the presence of a two-helix junction and sequence similarity in the three binding sites (Fig. 9), mimicry between operator binding site 1 and the L20-binding site on 23S rRNA is maybe less evident than that with operator binding site 2 because of the pseudoknotted nature of binding site 1. Therefore, we cannot exclude the possibility that L20 has a second RNA-binding site that recognizes binding site 1 differently from 23S rRNA and operator binding site 2. In this case, a single L20 molecule would suffice to bind the two sites of the *rpmI* translational operator. The X-ray structure of the large ribosomal subunit of *D. radiodurans* shows that not only the C-terminal globular domain of L20 but also its N-terminal domain makes extensive contacts with 23S rRNA (Harms et al., 2001). One hypothesis would be that L20 binds to sites 1 and 2 of mRNA the same way it binds 23S rRNA, that is, the L20 C-terminal domain binds to site 2 by mimicking its interaction with its binding site on 23S rRNA and the N-terminal domain of the protein interacts with site 1. However, it has been shown that the C-terminal domain of the protein is sufficient to repress the expression of *rpmI* in vivo (Raibaud et al., submitted), thus making this hypothesis unlikely. For that reason we rather favor a scenario in which two L20 molecules bind to mRNA through interaction of their C-terminal domains with sites 1 and 2.

MATERIALS AND METHODS

Site-directed mutagenesis

Two complementary primers containing the desired mutation or deletion were extended by *Pfu* DNA polymerase using the replicative form of M13mp18MQ21ΔNB DNA as template according to the QuickChange Site-Directed Mutagenesis Kit (Stratagene). M13mp18MQ21ΔNB is a M13mp18 derivative carrying the *rpmI'-'lacZ*α translational fusion expressed from the p_1 promoter of the IF3 operon (Lesage et al., 1992). It carries all the *cis*-acting sequences (the *rpmI* translational operator) required for repression of *rpmI* expression by L20. Sequences of the oligonucleotides are available upon request. The presence of all mutations and deletions was confirmed using the dideoxy chain termination method (Sanger et al., 1977).

Plasmid construction

Plasmids pOT, pOTΔinfC331–337, pOT iris 53–55 and pOTΔApaLI were constructed by cloning the *Eco*RI-

*Bam*HI fragment of the replicative form of the appropriate M13mp18MQ21ΔNB DNA derivative downstream of a phage T7 promoter in pBlueScript-SK(+). M13mp18MQ21 (ΔApaLI)ΔNB containing a deletion between nucleotides residues infC A365 and C521 has been previously described (Chiaruttini et al., 1996). Deletion in M13mp18MQ21 (ΔinfC331–337)ΔNB and point mutations in M13mp18MQ21 (iris 53–55)ΔNB were introduced in this work.

Preparation of transcripts containing the *rpm*I translational operator

First, plasmids were linearized by *Nco*I, which cleaves at position 143 of *rpmI*, and then used as templates in in vitro transcription reactions using T7 RNA polymerase as recommended by the manufacturer (Promega). Transcription starts upstream to the p1 promoter of the IF3 operon. Henceforth, the transcripts will be referred to as *rpm*I translational operators. Plasmid pTZΔ20-10, which carries all the sequences required for translational repression of *thrS* expression by ThrRS (Brunel et al., 1992), was cleaved with *Ssp*I and used as template for transcription with T7 RNA polymerase. The resulting transcript is henceforth referred to as the *thrS* translational operator.

Preparation of phosphorothioate-substituted transcripts containing the *rpm*I translational operator

*Nco*I-linearized plasmid pOTΔApaLI was used as template in four transcription reactions with T7 RNA polymerase in which one of the four NTPs was supplemented by the corresponding NTP[αS]. Transcription reactions were performed essentially as described in Schatz et al. (1991) except that NTP[αS]/NTP molar ratio was 1% instead of 5%.

Preparation of *E. coli* L20

L20 was expressed from plasmid pUA6 (Lesage et al., 1990) transformed into *E. coli* JM109. This high-copy number plasmid carries the *E. coli rplT* gene under the control of a lac promoter. Cells were grown at 37 °C in 2XTY medium containing ampicillin and induced with 1 mM IPTG overnight when they reached an OD_{650} of 0.4. They were spun down, washed with buffer A (10 mM Tris-HCl, pH 7.4, 60 mM NH_4-acetate, 10 mM Mg-acetate, 6 mM β-mercaptoethanol), spun down again, frozen at −80 °C and then disrupted by grinding with alumina. After suspension in buffer A, undisrupted cells and cellular debris were removed by centrifugation. The supernatant was centrifuged at 105,000 × *g* for 3 h at 4 °C and the pellet was suspended in buffer B (6 M urea, 50 mM NH_4-acetate, pH 5.6, 6 mM β-mercaptoethanol). The suspension was extracted with 6 M LiCl and 2 M urea on ice overnight, centrifuged, and the supernatant was dialyzed overnight against buffer B. L20 was purified by ion-exchange chromatography at room temperature on a Mono S (10/10) FPLC column (Amersham Pharmacia Biotech) using a 0.3 M to 1 M linear NaCl gradient made in buffer B. Under these conditions, L20 eluted at 0.6 M NaCl. L20-containing fractions were collected and dialyzed at 4 °C for 1 h against 2,000 vol of water and then for 2 h against 400 vol of 50% glycerol, 50 mM K-phosphate, pH 7.5, 1 mM EDTA.

DMS and CMCT footprinting experiments

Modifications of the *rpm*I translational operator were performed with DMS and CMCT. First, the operator (500 fmol) in 7 μL of either DMS (50 mM Na-cacodylate, pH 7.5) or CMCT (50 mM Na-borate, pH 8.0) buffer was denatured by heating at 80 °C for 3 min followed by immediate cooling in ethanol containing solid CO_2. Samples were thawed on ice and Mg-acetate in 1 μL of either DMS or CMCT buffer was added to a final concentration of 10 mM. L20 (15 pmol) in 1 μL of either DMS or CMCT buffer supplemented with Mg-acetate was then added. The L20/operator molar ratio was 30. The samples were incubated at 37 °C for 10 min and cooled at room temperature for 15 min. DMS or CMCT in 1 μL of the corresponding buffer supplemented with Mg-acetate was added to a final concentration of 0.25% (v/v) for DMS and 0.01% (w/v) for CMCT. Modifications were carried out at room temperature for 3 min with DMS and 15 min with CMCT and stopped by ethanol precipitation with 2.5 μg of *Lactococcus lactis* 23S rRNA. Transcripts were suspended in 50 μL of 20 mM Tris-HCl, pH 7.5, 5 mM EDTA, 0.5% SDS, and proteinase K was added at a final concentration of 1 μg/μL. Proteinase K treatment was at 37 °C for 15 min. Transcripts were purified by phenol extraction, and the sites of modification were determined by extension of 5′-end-labeled rpmI84 or rpmISD primer. Extension products were analyzed by gel electrophoresis, essentially as described in Chiaruttini et al. (1996). The gels were scanned using a PhosphorImager (Molecular Dynamics). The sequences and complementarities of the primers are as follows: rpmI84 (5′-GGTCAGAATGTGACGCAG-3′) is complementary to positions 102 to 85 in *rpmI*, and rpmISD (5′-AATAACTTCCACTTCGC-3′) is complementary to positions 93 to 77 in iris.

Iodine footprinting experiments

Each of the four phosphorothioate-substituted transcripts (500 fmol) in 7 μL of TN buffer (10 mM Tris-acetate, pH 7.5, 60 mM NH_4Cl) was denatured as described above and Mg-acetate in 1 μL of TN buffer was added to a final concentration of 10 mM. L20 (15 pmol) in 1 μL of TN buffer supplemented with Mg-acetate was then added and the samples were incubated at 37 °C and then cooled as described above. The L20/operator molar ratio was 30. Iodine in 1 μL of ethanol was added to a final concentration of 1 mM. The four samples were incubated at room temperature for 1 min and the reaction was stopped by ethanol precipitation with 2.5 μg of *L. lactis* 23S rRNA. Samples were then submitted to proteinase K treatment and primer extension as described above. Extension products were analyzed by gel electrophoresis and the gels scanned as described above.

L20-induced primer extension arrest

The *rpmI* and *thrS* translational operators were used to extend the rpmI84 and M13-17mer primers, respectively. The sequence of rpmI84 primer has been given above. M13 17-mer primer is complementary to sequences in *lacZ* down-

stream of the *thrS* translational operator cloned into pTZΔ20-10. Its sequence is 5′-GTAAAACGACGGCCAGT-3′. The operator (50 fmol) and the appropriate 5′-end-labeled primer (150 fmol) were mixed in 7 μL of SB solution (TN buffer supplemented by 6 mM β-mercaptoethanol). The mixture was heated at 80 °C for 3 min and immediately cooled in ethanol containing solid CO_2. The mixture was thawed on ice, and Mg-acetate in 1 μL of SB buffer was added to a final concentration of 10 mM. L20 (1.5 pmol) in 1 μL of SBM buffer (SB buffer supplemented by 10 mM Mg-acetate) was then added, and the samples were incubated at 37 °C for 10 min. The L20/*rpmI* or *thrS* translational operator molar ratio was 30. The four dNTPs, together with 1 U of AMV RT in 1 μL of SBM buffer, were added to a final concentration of 375 mM, followed by incubation at 37 °C for an additional 15 min. Extension products were analyzed by gel electrophoresis and the gels scanned as described above.

Lambda bacteriophages, translational fusions, and *E. coli* lysogens

Mutant derivatives of M13mp18MQ21ΔNB were cloned into λ as described (Lesage, 1992 #839). Lysogenization of *E. coli* IBPC5311, monolysogen screenings, growth conditions of plasmid-carrying monolysogens and β-galactosidase measurements were as described (Springer et al., 1985, 1986; Lesage et al., 1992). In these fusions, *lacZ* was fused in phase with the first 157 nt of *rpmI.*

ACKNOWLEDGMENTS

We are indebted to C. Condon for critical reading of the manuscript and helpful suggestions. We thank Michèle Milet for help with modification experiments. This work was supported by grants from the Centre National de la Recherche Scientifique (CNRS; Unité Propre de Recherche 9073) and the CNRS "Physique et Chimie du Vivant" program. M.G. and S.R. were recipients of studentships from the French Ministry of Research.

Received March 14, 2002; returned for revision April 11, 2002; revised manuscript received April 29, 2002

REFERENCES

Brunel C, Caillet J, Lesage P, Graffe M, Dondon J, Moine H, Romby P, Ehresmann C, Ehresmann B, Grunberg-Manago M, Springer M. 1992. The domains of the *E. coli* threonyl-tRNA synthetase translational operator and their relation to threonine tRNA isoacceptors. *J Mol Biol 227*:621–634.

Butler JS, Springer M, Dondon J, Graffe M, Grunberg-Manago M. 1986. *Escherichia coli* protein synthesis initiation factor IF3 controls its own gene expression at the translational level in vivo. *J Mol Biol 192*:767–780.

Chiaruttini C, Milet M, Springer M. 1996. A long-range RNA–RNA interaction forms a pseudoknot required for translational control of the IF3-L35-L20 ribosomal protein operon in *Escherichia coli*. *EMBO J 15*:4402–4413.

Gregory RJ, Cahill PBF, Thurlow DL, Zimmermann RA. 1988. Interaction of *E. coli* ribosomal protein S8 with its binding sites in ribosomal RNA and messenger RNA. *J Mol Biol 204*:295–307.

Harms J, Schluenzen F, Zarivach R, Bashan A, Gat S, Agmon I, Bartels H, Franceschi F, Yonath A. 2001. High resolution structure of the large ribosomal subunit from a mesophilic eubacterium. *Cell 107*:679–688.

Köhrer C, Mayer C, Neumair O, Gröbner P, Piendl W. 1998. Interaction of ribosomal L1 proteins from mesophilic and thermophilic Archaea and Bacteria with specific L1-binding sites on 23S rRNA and mRNA. *Eur J Biochem 256*:97–105

Lesage P, Chiaruttini C, Graffe M, Dondon J, Milet M, Springer M. 1992. Messenger RNA secondary structure and translational coupling in the *Escherichia coli* operon encoding translation initiation factor IF3 and the ribosomal proteins, L35 and L20. *J Mol Biol 228*:366–386.

Lesage P, Truong HN, Graffe M, Dondon J, Springer M. 1990. Translated translational operator in *Escherichia coli*: Autoregulation in the *infC-rpmI-rplT* operon. *J Mol Biol 213*:465–475.

Nomura M, Gourse R, Baughman G. 1984. Regulation of the synthesis of ribosomes and ribosomal components. *Ann Rev Biochem 53*:73–117.

Nomura M, Yates JL, Dean D, Post LE. 1980. Feedback regulation of ribosomal protein gene expression in *E. coli*: Structural homology of ribosomal RNA and ribosomal protein mRNA. *Proc Natl Acad Sci USA 77*:7084–7088.

Said B, Cole JR, Nomura M. 1988. Mutational analysis of the L1 binding site of 23S rRNA in *Escherichia coli*. *Nucleic Acids Res 22*:10529–10545.

Sanger F, Nicklen S, Coulson AR. 1977. DNA sequencing with chain-terminating inhibitors. *Proc Natl Acad Sci USA 74*:5463–5467.

Schatz D, Leberman R, Eckstein F. 1991. Interaction of *Escherichia coli* $tRNA^{Ser}$ with its cognate aminoacyl-tRNA synthetase as determined by footprinting with phosphorothioate-containing tRNA transcripts. *Proc Natl Acad Sci USA 88*:6132–6136.

Springer M, Graffe M, Butler JS, Grunberg-Manago M. 1986. Genetic definition of the translational operator of the threonine tRNA ligase gene in *Escherichia coli*. *Proc Natl Acad Sci USA 83*:4384–4388.

Springer M, Plumbridge JA, Butler JS, Graffe M, Dondon J, Mayaux JF, Fayat G, Lestienne P, Blanquet S, Grunberg-Manago M. 1985. Autogenous control of *Escherichia coli* threonyl-tRNA synthetase expression in vivo. *J Mol Biol 185*:93–104.

Springer M, Portier C, Grunberg-Manago M. 1998. RNA mimicry in the translational apparatus. In: Simon RW, Grunberg-Manago M, eds. *RNA structure and function*. Cold Spring Harbor, New York: Cold Spring Harbor Laboratory Press. pp 377–413.

Wower I, Kowaleski MP, Sears LE, Zimmermann RA. 1992. Mutagenesis of ribosomal protein-S8 from *Escherichia coli*: Defects in regulation of the *spc* operon. *J Bacteriol 174*:1213–1221.

Wu H, Jiang L, Zimmermann RA. 1994. The binding site for ribosomal protein S8 in 16S rRNA and *spc* mRNA from *E. coli*: Minimum structural requirements and the effects of single bulged bases on S8-RNA interaction. *Nucleic Acids Res 22*:1687–1695.

Zengel JM, Lindahl L. 1994. Diverse mechanisms for regulating ribosomal protein synthesis in *E. coli*. *Prog Nucleic Acid Res Mol Biol 47*:331–369.